D-Microfibers

Felipe Beltrán-Mejía, *Member, IEEE, OSA*, Jonas H. Osório, Claudecir R. Biazoli, and Cristiano M. B. Cordeiro

***Abstract*—A simple mechanical setup was used to polish a standard single mode optical fiber in order to make it asymmetric. The polished fiber was tapered down maintaining the D-shape transversal profile. Its broken symmetry along with the extended evanescent field, due to the dimensions of the microfiber, implies a potentially high birefringent waveguide as well as a high-sensitivity external refractive index device. An experimental maximum sensitivity of $S \approx (3.0 \pm 0.2) \times 10^4$ nm/RIU was achieved, other experimental and numerical results supporting our initial assumptions are also presented.**

***Index Terms*—Birefringence, microoptics, microsensors, optical fiber sensors, sensitivity, sensors.**

I. Introduction

OPTICAL fibers tinkered as birefringent waveguides are widely used to maintain the polarization state or for breaking the degeneracy of a propagation mode in telecommunications, nonlinear and sensing applications. All-solid polarization maintaining optical fibers (PMF) are fabricated by increasing the asymmetry (e.g., elliptical core fibers) to induce a form birefringence or by introducing different materials at opposite sides of the cladding to induce a stress birefringence. In consequence, the effective refractive index inside the core is different for the different polarization states, creating a high birefringent waveguide. Also, photonic crystal fibers, optical fibers surrounded by an array of airholes extending down the fiber length, have demonstrated to be an order of magnitude more birefringent than the all-solid PMF fibers [1], [2]. Their geometrical richness enables a more accurate control of the dispersion profile for both polarization states, albeit a more complex fabrication process is needed in order to fabricate the microstructure of air-holes inside the fiber cladding.

Recently, subwavelength diameter fibers (microfibers) have been proposed as an appealing alternative for high birefringent waveguiding and as a high sensitive solution due to their low loss and high evanescent fields. By tapering down a rectangular silica preform, high values have been reported for both, group birefringence [3] and external refractive index sensitivities as high as 2.06×10^4 nm/RIU [4]. But to obtain such tailored preforms with a rectangular cladding may not be easy as it implies all the inconveniences of the preform shaping and the drawing process, while avoiding strain rounding effects. As an alternative, a small extent of the cladding of a conventional fiber could be casted into an oblong geometry and then tapered into sub-wavelength dimensions, as it has been done by laser-etching, reporting high values for group birefringence [5].

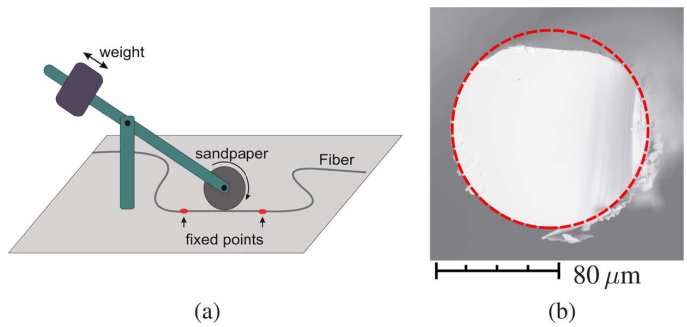

Fig. 1. (a) Experimental setup. A spinning cylinder, wrapped around with sandpaper, polishes the fiber fixed to a flat surface. (b) Optical microscopy image of a polished fiber previous to the tapering process. Debris can be seen close to the polished region. The polishing process typically lasted a few minutes.

In this paper we describe a simple mechanical setup used to polish standard single mode fibers (SMF-28) and taper them down in order to obtain high birefringence and high sensitivity in a D-shaped microfiber. Recently, a circular-symmetric microfiber isolated with a low index material all around except for the sensing region has been proposed promising high sensitivity [6]. In contrast, our proposal does not needs an extra isolation, making it simpler and more robust. Also, since the fiber's cross section has infinite rotation and reflection symmetries, we believe the break of symmetry will induce a greater birefringence in comparison with those obtained by breaking the finite symmetry of a squared preform. Even more, this could be achieved without the experimental complexity implicit in the construction of a rectangular microfiber. At the same time, the fiber's pigtails are standard single mode fibers, keeping all the advantages for low-loss fiber connectorization.

In what follows, the polishing method will be described in detail, followed by the experimental measurements and the numerical results obtained for phase and group birefringence and external refractive index sensitivity. Finally, the results are discussed leading to the conclusions of this proposal.

II. Experimental Methods

To cast a conventional fiber into a D-shape cross section profile, the fiber was fixed on a flat surface and then polished with a sandpaper (220 mesh) glued on the surface of a spinning cylinder. Special care had to be taken as to avoid bumps on the spinning surface, since that will result in an irregular polishing or, more probably, fracturing the fiber. Fig. 1(a) shows a schematic diagram for the employed polishing setup. As the fiber was polished, fiber cladding materials were partially

Manuscript received October 02, 2012; revised May 21, 2013; accepted July 08, 2013. Date of publication July 11, 2013; date of current version July 26, 2013. This work was supported in part by the São Paulo Research Foundation, under Grants 2011/01524-8 and 2010/13149-4.

The authors are with the Instituto de Fısica "Gleb Wataghin", Universidade Estadual de Campinas—UNICAMP, Campinas, SP, Brazil (e-mail: cmbc@ifi.unicamp.br).

Color versions of one or more of the figures in this paper are available online at http://ieeexplore.ieee.org.

Digital Object Identifier 10.1109/JLT.2013.2272915

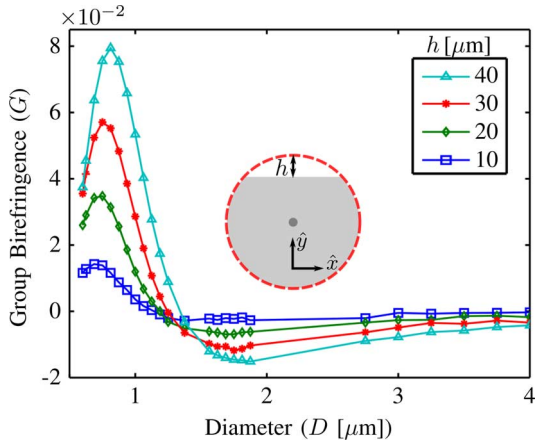

Fig. 2. Numerical simulations for the group birefringence using different polishing depths (h, as shown in the legend) and air as the external refractive index. The inset shows a schematic drawing of a polished fiber cross section, while the diameter is the same as for a non-polished fiber.

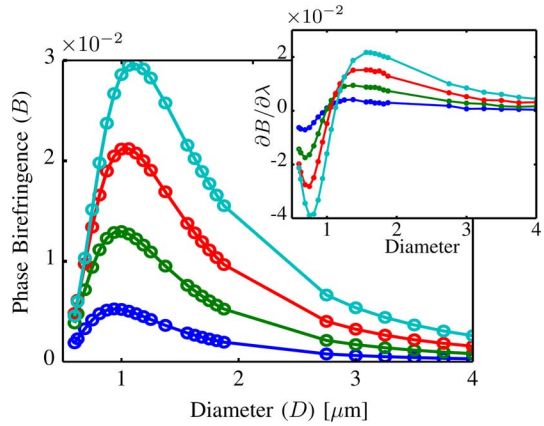

Fig. 3. Numerical results for the phase birefringence B using different polishing depths h and air as the external material. The inset shows the derivative $\partial B/\partial\lambda$ as a function of the fiber's diameter. For both graphs the color legend is the same as in Fig. 2.

removed, losing the circular symmetry of the fiber cross section (Fig. 1(b)). As shown, a counterweight was used to balance the weight of the spinning cylinder and avoid an excessive tensile stress over the optical fiber. However, when the fiber is at its nominal diameter ($D = 125$ μm), the birefringence induced by the broken symmetry is negligible since the light is confined inside the core.

In order to obtain optical microfibers with high birefringence, the polished fibers were tapered down using the flame brushing technique [7]. In this technique, a well defined region of the fiber has its dimensions decreased by a factor that can be chosen to be up to 200 times. To perform the process, the fiber had its extremities attached to two translation stages able to longitudinally stretch the fiber. Besides, this technique employs a flame (also connected to a translation stage) that oscillates below the fiber in order to heat it, causing its viscosity to decrease. Therefore, as the heated fiber was stretched, by mass conservation its length increased as its diameter decreased.

Due to the narrow taper waist, light will no longer be confined inside the core. Instead, light will be guided through the entire cross section of the microfiber—including the cladding—as a consequence of the refractive index difference between air and silica. In addition, as a result of the D-microfiber's cross section, different effective indexes are obtained for both directions, parallel and perpendicular to the normal direction of the polished region (as shown by the coordinate axes at the inset of Fig. 2). Then, the degeneracy of the orthogonal states is broken, that is, the microfiber is now birefringent.

The D-shape of the microfiber was maintained while the fiber was tapered. Otherwise, the microfiber would no longer be birefringent since the geometrical asymmetry is responsible for the birefringence of the waveguide. As will be presented in the next section, we performed measurements during the taper fabrication and observed interference due to the recombination of the modes that traveled through the fiber with different polarizations. Thus, as the interference can only happen if the fiber is birefringent, one can infer that the D-shape was maintained while the fiber was stretched.

III. Numerical and Experimental Results

Before tackling the simulation of the D-microfiber, the results presented for group birefringence in [3] and sensitivity in [4] were reproduced using a commercial finite-element software. Furthermore, since the group birefringence,

$$G(\lambda) = B(\lambda) - \lambda\frac{\partial B}{\partial \lambda}. \tag{1}$$

depends on the derivative of the phase birefringence, B, relative to the wavelength, λ, special care had to be taken when calculating G. An important source of error could arise if truncation and roundoff errors are not considered, as for example, when calculating the numerical derivative $\partial B/\partial\lambda$ for fibers with a small polishing depth. For this reason, a modal iterative Fourier method [8] was used in order to cross-check our results. This latter method incorporates an analytic procedure to calculate $\partial B/\partial\lambda$, which let us calculate G semi-analytically, avoiding the implicit error when calculating the numerical derivatives [9]. Good resemblance between the results of both methods, and the results reported by other authors validates our analysis.

The remainder of this section will present the results for the group birefringence and the sensitivity for the external refractive index, S, of the proposed D-microfiber. First, we will show how this simple experimental proposal can attain ultra-high birefringence values. Followed by the results obtained using the D-microfiber as a highly sensitive device for detecting variations in the outer refractive index. In both cases numerical results and experimental measurements are presented for comparison and to show the high potential the D-microfiber has as a high birefringent waveguide.

1) Group Birefringence: The group birefringence of the fundamental mode was studied as the fiber diameter decreases as in the tapering process. As shown on the inset of Fig. 2, the fiber cross section was approximated to a D-profile, although the polished region previous to the tapering process was not as regular (see Fig. 1(b)). On Fig. 3, as expected, the phase birefringence reaches a peak value when the light is well confined in the $\hat{x}$ direction and highly evanescent in $\hat{y}$ direction. This same behavior was found for G in Fig. 2, showing how by polishing

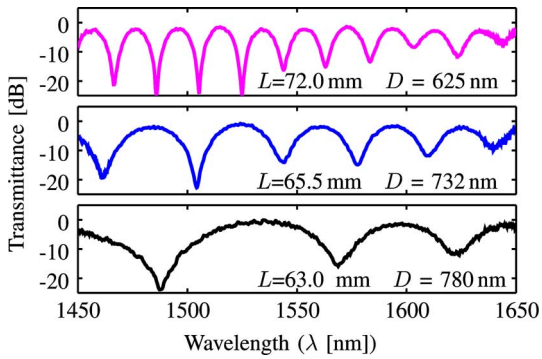

Fig. 4. Transmittance spectra for a D-microfiber surrounded by air as the tapering process reduced its nominal diameter. Notice how the FSR decreased as the diameter was reduced and the taper stretched. For each spectra, the geometrical parameters are as presented in Table I.

deeper—augmenting h—higher values for the birefringence can be attained. Maximum group birefringence of approximately 1.4×10^{-2} and 8.1×10^{-2} were achieved for a 10 μm and 40 μm polished fibers with a 0.75 μm and 0.79 μm diameter, respectively. Notice also the sign of G is determined by the relation between B and $\partial B/\partial\lambda$, as can be seen by comparing Figs. 2 and 3. The change of signal when G crosses the horizontal axis $G=0$ will have a crucial role in the next section, where we explore the properties of the D-microfiber as a sensing application.

The measurements for the group birefringence were done using the wavelength-scanning method [10], where input light polarized at 45° was filtered by a second polarizer with the same orientation but at the output end resulting in an intensity periodic pattern as shown in Fig. 4 for different taper lengths—geometrical data concerning the fiber tapers whose spectra are shown in Fig. 4 are presented in Table I. The group birefringence was obtained using the expression,

$$G=\frac{\lambda^2}{PL}, \tag{2}$$

where P is the Free Spectral Range (FSR)—distance between peaks—and L is the extension of the birefringent waveguide. We assumed that the taper waist acts as a birefringent fiber and used its length as L to estimate the group birefringence. Nevertheless, the polished region could be longer or shorter than the taper waist. Then, some extent of the transition region between the initial fiber and the taper waist may also be birefringent or the polished region could be shorter than the taper length. Since the determination of L is a difficult task, we believe it is an important source of error concerning the experimental data. Also, a maximum insertion loss of 5 dB was estimated for the fabricated birefringent microfiber comparing the transmittance between the fiber at its nominal diameter and after the fiber was tapered.

Apart the dependence of G with the waveguide length, the external refractive index also plays an important role. As discussed in the next section, the general trend as the external refractive index increases, is a less confined optical field inside the fiber core and, therefore, a decremented G. In some configurations P—the fringe period or FSR—can be too long and difficult to be quantified, possible solutions include using optical sources with broader band and/or longer taper waists.

TABLE I
DIAMETER (D), TAPER LENGTH (L) AND TRANSITION REGION LENGTH (Z) FOR THE DIFFERENT TAPERED FIBERS USED IN FIG. 4

D [nm]	L [mm]	Z [mm]
625	72.0	40.0
732	65.5	36.0
780	63.0	35.0

Diameter (D), taper length (L) and transition region length (Z) for the different tapered fibers used in Fig. 4.

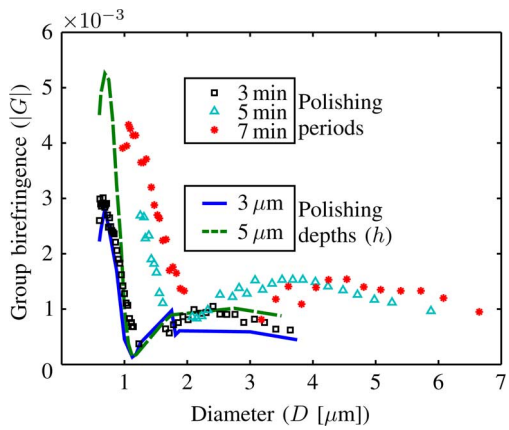

Fig. 5. Experimental results (colored marks) for the absolute value of G using different polishing times and air as the external material. Numerical results (colored curves) are for the same fiber cross section as in Fig. 2, using $h=3$ and 5 μm as polishing depths and represented as solid and dashed lines respectively.

Fig. 5 compares experimental and numerical results for the absolute value of the group birefringence as a function of the taper diameter. As shown in the upper legend, the different colored markers represent fibers polished during different periods of time, all of them have an approximately 2.5 cm long polished section. The solid and dashed lines represent the birefringence obtained for two ideal D-microfibers with different polishing depths, 3 and 5 μm respectively. One could observe that a correct behavior for the dependence of G with D was obtained. Also, it can be estimated that the polishing depths h of the experimental results were between 3 and 5 μm as used on the numerical analysis.

The behavior of the curves in Figs. 2 and 5 is better understood in view of (1) and Fig. 3. As shown in Fig. 2, when D is higher than 2 μm, G becomes negative and a local critical value is obtained. As can be seen in Fig. 3, for those values of D, a low valued B together with a considerable $\partial B/\partial\lambda$ makes the second term in (1) prevails. For smaller values of D, the phase birefringence is maximum when the diameter is close to the value of λ. Close to this point, the derivative $\partial B/\partial\lambda$ is negative and both terms in (1) add up to reach a maximum value for G. As expected, a final drop occurs—for both B and G—when the wavelength exceeds the waveguide dimensions and the breakage of the symmetry has almost no effect.

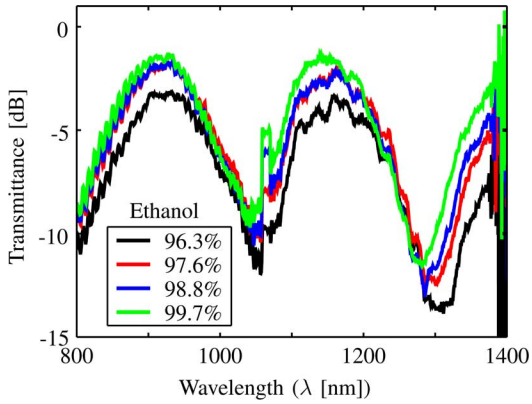

Fig. 6. Transmittance peaks for a 4 μm thick D-microfiber with different external refractive indexes represented as different concentrations of alcohol in water, as shown in the legend. Taper and transition region length equal to $L = 140.5$ mm and $Z = 34$ mm, respectively.

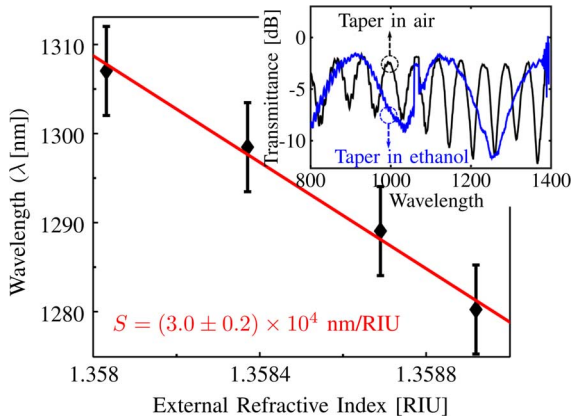

Fig. 7. Measurements of the peak displacements when varying the external refractive index, as in Fig. 6. The slope of the linear fit is equivalent to the measured sensitivity, $S = (3.0 \pm 0.2) \times 10^4$ nm/RIU. Inset shows the transmission spectra for a 4 μm thick D-microfiber surrounded by air and ethanol.

The experimental values for the taper waist diameter (D) were calculated by using the expression reported by [7],

$$D = D_0 \left[1 + \frac{\alpha x}{L_0}\right]^{-\frac{1}{2\alpha}}, \tag{3}$$

where D_0 is the original fiber diameter (125 μm), α is a constant that takes into account the relative rates of flame oscillation and the elongation of the taper, x is the longitudinal displacement of the translation stage to which the fiber is attached and L_0 is the initial heated region length.

As the setup for producing the fiber taper was computer controlled (α and L_0 were parameters set by the user and x was taken into account by observing the stages displacement), the D value was calculated during the taper fabrication process. Then, the instantaneous diameter of the fiber taper waist is known. It is important to analyze, however, that there may be errors concerning the D value, since the derivation of the expression presented above takes into account a cylindrically symmetric optical fiber—what is not true for the side polished optical fibers. Besides, as it is possible to know the instantaneous taper diameter while the taper is produced, for the group birefringence measurements as a function of the fiber diameter, it was not necessary to take the taper out of the setup for taking measurements. The fiber extremities were previously connected to a broadband light source (superluminescent light emitting diode) and to an optical spectrum analyzer; thus, while the taper fabrication was running, the spectra could be recorded.

2) Sensitivity: The sensitivity, defined as the dependency of the transmittance spectra with the external refractive index, was experimentally measured in the same way as in [4]. That is, on a transmittance graph (see Fig. 6), the displacement of the peaks λ_t—due to the variation of the external refractive index (n_{ext})—were fitted to a line whose slope represents the sensitivity, as shown in Fig. 7. The spectral position of the peak centered at $\lambda \approx 1307$ nm was followed as the refractive index of the external medium was varied. Selecting this particular value for λ was by reason of a better defined peak at this wavelength.

In Fig. 6, the presented transmission spectra show how the D-microfiber is sensitive to small additions of ethanol in water. A change of roughly 1% of the concentration implies a considerable shift of the peak position, λ_t. In order to perform this measurement, the fiber taper was carefully put in a box filled with ethanol-water solutions with different concentrations, providing changes in the external refractive index.

The peaks displacements as a function of the external refractive index are represented in a λ_t vs. n_{ext} graph as in Fig. 7. Finally, the slope obtained from the linear fit (solid red line) gives the experimental measurement of the sensitivity, S, for a determined central wavelength and a external refractive index. Using this method, a maximum sensitivity of $(3.0 \pm 0.2) \times 10^4$ nm/RIU was obtained. This value for the sensitivity has the same magnitude order as the one obtained by Jie Li *et al.* in [4].

The inset in Fig. 7 shows how the transmission spectrum changes abruptly when the fiber taper was immersed in air and in ethanol. This variation is explained by the fact that the group birefringence was lower when the fiber was immersed in a medium of higher refractive index. Also, it should be pointed out that the wavelength bandwidths from measurements in Fig. 4 differs from those in Figs. 6 and 7 as a reason of the peak's broadening when the fiber tapers were immersed in water-ethanol solutions. As can be seen in Fig. 6, a 200 nm optical window will be insufficient for the FSR measurement. Also, at wavelengths above 1400 nm a low transmittance was obtained due to water absorption. Thus, it was necessary to change the wavelength bandwidth to perform the sensing measurements.

The sensitivity can be defined as $d\lambda_t/dn_{\text{ext}}$, that after an expansion around a small variation can be approximated as,

$$S \approx \frac{\lambda}{G} \frac{\partial B}{\partial n_{\text{ext}}} \tag{4}$$

where λ is the vacuum wavelength at which G and $\partial B/\partial n_{\text{ext}}$ were calculated. The external refractive indexes n_{ext} were estimated using the expression presented in [11]—for the refractive index of the mixture of two liquids—and the values of the refractive index of alcohol and water, 1.359 and 1.333 respectively [12].

From (4), it can be seen the sign of S is determined by the direction in which the peaks are shifted, being only of interest the

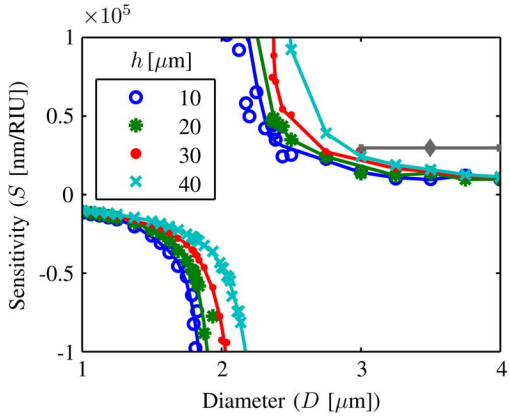

Fig. 8. Results for the proposed external refractive index microsensor for $n_{\text{ext}} = 1.3585$ RIU and $\lambda = 1.295$ μm. Colored marks represents the numerical results for S using different polishing depths, h, as shown in the legend. A polynomial fit is presented as solid lines to aid the eye. The experimental result obtained for a D-microfiber, with approximately $h \approx 15$ μm and a diameter of 3.5 ± 0.5 μm, are represented by a gray rhombus and its error bar.

absolute value of S. When the microfiber waist and the external refractive index are related in a way that G is close to zero, maximum values of $|S|$ are obtained. For that reason, to accurately measure P for low values of G, one must obtain the longer fiber taper possible, as it is supported by (2).

The numerical results obtained for the sensitivity are presented in Fig. 8, where colored marks represent the numerical results and the solid colored lines are polynomial fits drawn to aid the eye and show the tendency of the results. On the right side of Fig. 8, the solid gray rhombus represents the experimental measurement, $S = (3.0 \pm 0.2) \times 10^4$ nm/RIU. Both numerical and experimental results were made using external refractive indexes around $n_{\text{ext}} = 1.3585$ RIU and wavelengths around $\lambda = 1.15$ μm.

IV. Conclusion

The D-microfiber has demonstrated to be a successful proposal as an ultra-high birefringent waveguide as well as a highly-sensitive external refractive index microsensor. Our initial hypothesis can be confirmed by comparing the values of the group birefringence for the D-microfiber with those of the rectangular microfiber using the same diameters. A higher G was obtained by using similar dimensions while the D-microfiber uses a standard SMF-28 fiber avoiding the fabrication of specially designed preforms. This also signifies a better compatibility with other connectorized fiber components.

The D-microfiber is a viable proposal as high birefringence can be achieved without polishing too deep. As shown in Fig. 2 a polishing depth of just 10 μm will be enough to attain a birefringence superior to 10^{-2}. It can also be noticed a right shift of the maxima of each curve as h increases, this is due to the different dimensions in the parallel (x axis) and transversal direction (y axis) of the polished section. In other words, a deep polished fiber needs to be less tapered to obtain a maximum G, that is because the y polarized field will be highly evanescent much sooner—as D decreases—than the x polarized field. After this maxima was attained, further reducing the taper dimensions made both fields evanescent, the asymmetry of the waveguide became irrelevant and therefore G drops drastically.

Fig. 5 shows an agreement between the measured G and the simulations. Qualitatively, the same trends—the maxima, the minima and the roots—of the function G were observed for both the numerical and experimental results. Discrepancy may be caused by the approximation of the fiber profile to an ideal D-shaped microfiber. Also, as already discussed, determining the length L of the tapered polished region as it appears in (2), may be an important source of error.

On the other hand, in the case of the sensitivity, polishing too deep can make the D-microfiber very brittle, at a point it can be broken just by the superficial tension of the outer liquid. To circumvent this drawback, it is possible to polish under 10 μm and select the appropriate taper diameter in order to make G close to zero. As it can be seen from (4), the point where $G \approx 0$ determines the diameter of the taper at which $|S|$ is boosted. In that way, the polishing could be superficial and, at the same time, attain values over 10^5 nm/RIU for the sensitivity (Fig. 8).

Finally, as future perspectives, there is a need to improve our experimental techniques in order to enhance the control of parameters such as L and h. This will improve the accuracy as well as the reproducibility of our measures. It may also be interesting to use this polishing technique with a doubly-clad fiber. In this way, the inner clad will be exposed in one direction, while a tight confinement will be present at the other direction.

Acknowledgment

The authors would like to thank E. Silvestre for letting them make use of the iterative modal solver developed by his group [8] and for the advice on important points regarding these calculations.

References

[1] A. Ortigosa-Blanch, J. C. Knight, W. J. Wadsworth, J. Arriaga, B. J. Mangan, T. A. Birks, and P. S. J. Russell, "Highly birefringent photonic crystal fibers," *Opt. Lett.* vol. 25, no. 18, pp. 1325–1327, Sept. 2000 [Online]. Available: http://ol.osa.org/abstract.cfm?URI=ol-25-18-1325

[2] F. Beltrán-Mejıa, G. Chesini, E. Silvestre, A. K. George, J. C. Knight, and C. M. Cordeiro, "Ultrahigh-birefringent squeezed lattice photonic crystal fiber with rotated elliptical air holes," *Opt. Lett.* vol. 35, no. 4, pp. 544–546, Feb. 2010 [Online]. Available: http://ol.osa.org/abstract.cfm?URI=ol-35-4-544

[3] Y. Jung, G. Brambilla, K. Oh, and D. J. Richardson, "Highly birefringent silica microfiber," *Opt. Lett.* vol. 35, no. 3, pp. 378–380, Feb. 2010 [Online]. Available: http://ol.osa.org/abstract.cfm?URI=ol-35-3-378

[4] J. Li, L.-P. Sun, S. Gao, Z. Quan, Y.-L. Chang, Y. Ran, L. Jin, and B.-O. Guan, "Ultrasensitive refractive-index sensors based on rectangular silica microfibers," *Opt. Lett.* vol. 36, no. 18, pp. 3593–3595, Sep. 2011 [Online]. Available: http://ol.osa.org/abstract.cfm?URI=ol-36-18-3593

[5] H. Xuan, J. Ju, and W. Jin, "Highly birefringent optical microfibers," *Opt. Exp.* vol. 18, no. 4, pp. 3828–3839, Feb. 2010 [Online]. Available: http://www.opticsexpress.org/abstract.cfm?URI=oe-18-4-3828

[6] J.-L. Kou, Z.-D. Huang, G. Zhu, F. Xu, and Y.-Q. Lu, "Wave guiding properties and sensitivity of D-shaped optical fiber microwire devices," *Appl. Phys. B* vol. 102, pp. 615–619, 2011 [Online]. Available: http://dx.doi.org/10.1007/s00340-010-4244-y

[7] T. Birks and Y. Li, "The shape of fiber tapers," *J. Lightw. Technol.*, vol. 10, no. 4, pp. 432–438, 1992.

[8] E. Silvestre, T. Pinheiro-Ortega, P. Andrés, J. J. Miret, and A. Ortigosa-Blanch, "Analytical evaluation of chromatic dispersion in photonic crystal fibers," *Opt. Lett.* vol. 30, no. 5, pp. 453–455, Mar. 2005 [Online]. Available: http://ol.osa.org/abstract.cfm?URI=ol-30-5-453

[9] W. H. Press, S. A. Teukolsky, W. T. Vetterling, and B. P. Flannery, *Numerical Recipes in C (2nd Ed.): The Art of Scientific Computing*. New York, NY, USA: Cambridge Univ. Press, 1992.
[10] S. C. Rashleigh, "Measurement of fiber birefringence by wavelength scanning: Effect of dispersion," *Opt. Lett.* vol. 8, no. 6, pp. 336–338, Jun. 1983 [Online]. Available: http://ol.osa.org/abstract.cfm?URI=ol-8-6-336
[11] W. Heller, "Remarks on refractive index mixture rules," *J. Phys. Chem.* vol. 69, no. 4, pp. 1123–1129, 1965 [Online]. Available: http://pubs.acs.org/doi/abs/10.1021/j100888a006
[12] M. Astle and R. Weast, *CRC Handbook of Chemistry and Physics*. Boca Raton, FL, USA: CRC Press, 1979.

Author biographies not included at authors' request due to space constraints.